In-situ Full Scale Load Tests and Reliability Evaluation of Bearing Capacity for Nodular Cast-in-place Concrete Pile

K. Watanabe[1], A. Mitsumori[2], H. Nishioka[3] and M. Koda[4]
[1]*Geotechnical Engineering Department, Technical Research Institute, Obayashi Corporation, Tokyo, Japan*
[2]*Design Department, Obayashi Corporation, Tokyo, Japan*
[3]*Structures Technology Division, Railway Technical Research Institute, Tokyo, Japan*
E-mail: watanabe.koji.ro@obayashi.co.jp

ABSTRACT: In recent years, both the height and weight of buildings have increased. This trend is especially noticeable in the central urban areas of Japan. Both tensile and compressive forces occur in foundations such as these piles because of the overturning moment from earthquake and wind loads. To address these situations, new types of foundations need to be developed for high-rise superstructures. One approach is the nodular cast-in-place concrete pile, which has a nodular part at the mid-section of the pile. In situ full-scale load tests were carried out to estimate the bearing capacity of the nodular cast-in-place concrete pile. The bearing capacity was also estimated according to the Design Standards for Railway Structures and Commentary. This paper firstly summarizes the in-situ full scale load tests, and then describes the results of standard bearing capacity based on the data from the in situ full-scale load tests, finally mentions the estimation of ground resistance coefficient for nodular cast-in-place concrete piles.

KEYWORDS: Nodular cast-in-place concrete pile, In-situ full scale load test, Bearing capacity, Reliability evaluation

1. INTRODUCTION

Significant compressive and tensile forces due to both ordinary and earthquake loads act on the foundations of ultrahigh-rise buildings with large aspect ratios, which are increasing in number in the urban areas of Japan. A nodular cast-in-place concrete pile has been developed to handle this issue; this is a cast-in-place concrete pile with an increased diameter for the middle section containing a nodular part, as shown in Figure 1.

There have already been a number of applications in the architecture field (Watanabe, K. et al. 2008, Watanabe, K. et al. 2009, Watanabe, K. et al. 2010, Watanabe, K. et al. 2012). In the civil engineering field, when the space above railway tracks is utilized, the compressive force can be large because of the large spans, and the tensile force can be large because of high floor heights. This study evaluated the application of nodular cast-in-place concrete piles in civil engineering, particularly for the railway sector, with regard to their compliance with the Design Standards for Railway Structures (hereafter referred to as Railway Standards). This evaluation considered the variance in the bearing capacities of cast-in-place concrete piles and the different degrees of reaction forces for various displacement levels to reflect the above characteristics for end and nodular part resistances as well as the shaft resistance according to the standard pile end bearing capacity ratio. Establishing an evaluation method will make it possible to apply nodular cast-in-place concrete piles to railway structures.

This report outlines the load tests used for the evaluation and the results with regard to the degree of standard bearing capacity based on the load test data. The report also provides the results for the ground resistance coefficient, which is used to calculate the design bearing capacity.

2. CONSTRUCTION METHOD FOR CAST-IN-PLACE CONCRETE PILES

Figure 2 shows the construction procedure for nodular cast-in-place concrete piles. First, the hole for the shaft section is excavated using the earth drill construction method. The pile tip is then enlarged with further excavation. The nodular part section is then excavated using a special excavation device for the nodular part. Once the excavation is completed, the slime at the nodular part and pile tip sections is treated with slime cleaner. Then, the slurry in the cavities is replaced with a better liquid. Figure 3 shows a special slime cleaner that is used for the slime treatment of the nodular part sections. The steel reinforcement cage is then inserted, and the concrete is poured in a tremie pipe. The shape of the nodular part sections is verified by ultra sound measurements.

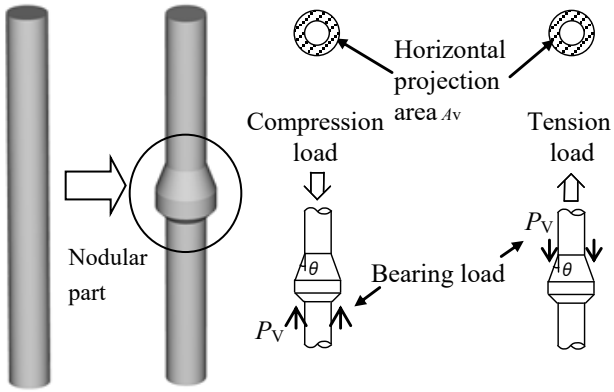

Figure 1 Schematic view of nodular cast-in-place concrete pile

3. IN SITU FULL-SCALE LOAD TEST FOR NODULAR CAST-IN-PLACE CONCRETE PILE

3.1 Outline

The load test data used for the evaluation were taken from two sites. All load tests were performed in compliance with the standard of the Japanese Geotechnical Society (Method for Axial Load Test of Single Piles). The loading continued until the displacement at the end of the pile exceeded 10% of the shaft diameter. The location of nodular part is determined the interlayer which has SPT N value larger than 20. The bearing capacity (i.e. bearing pressure) of the nodular part was calculated by dividing the difference in the axial forces above and below the nodular part by the horizontal projection area of the nodular part. The displacement of nodular part was defined as the displacement measured in the middle of the nodular part.

3.2 Load Test A

Figure 4 and Table 1 outline load test A. Two test piles were used with nodular part installed in the alluvial and diluvia sandy layers, which are representative bearing layers in the Osaka region, Japan. PC steel bars for tensile strength were installed at depths of up to

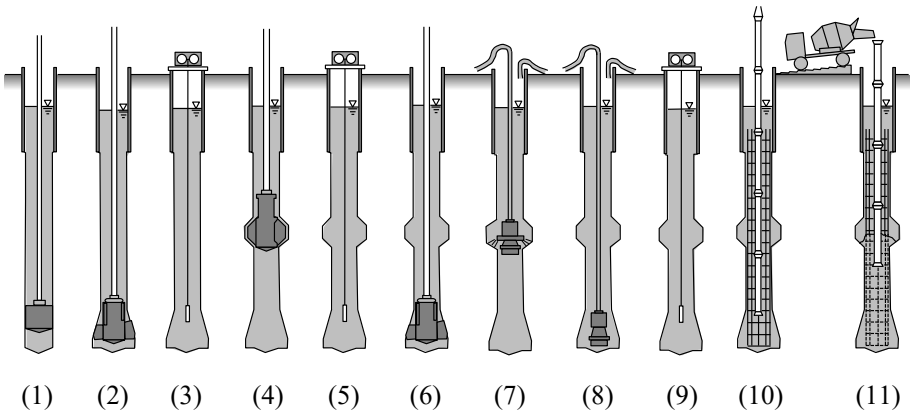

Procedure of construction
(1) Excavation of pile shaft
(2) Excavation of under-reamed part
(3) Measurement of pile shape
(4) Excavation of nodular part
(5) Measurement of pile shape
(6) Slime treatment
(7) Cleaning of nodular part
(8) Slime treatment
(9) Measurement of pile shape
(10) Insertion of steel reinforcement cage
(11) Concreting

Figure 2 Construction procedure of cast-in-place concrete pile

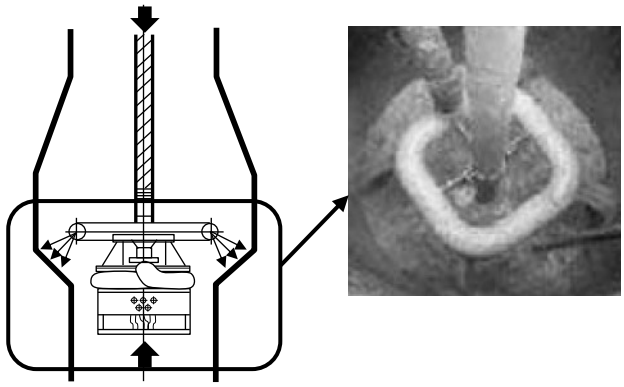

Figure 3 Slime cleaner for nodular part

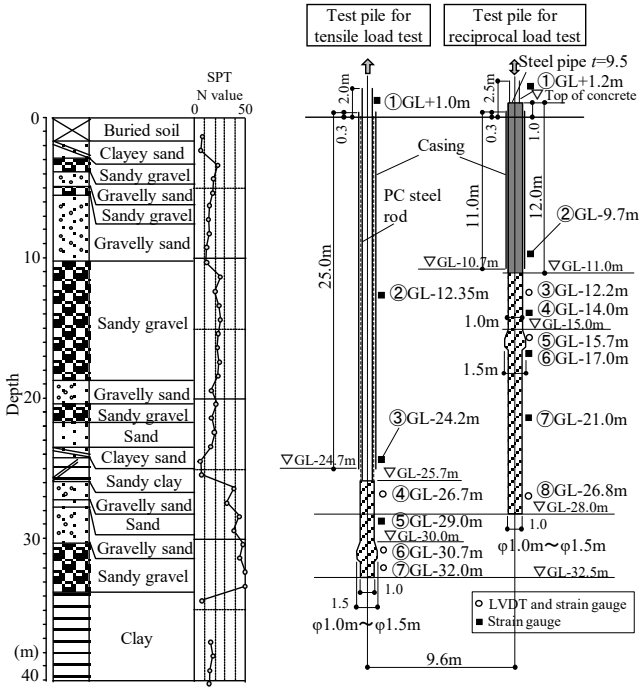

Figure 4 Summary of test piles and ground conditions (load test A)

Table 1 Specifications of test piles (load test A)

Load test	Pile length (m)	Depth of pile head (GL- m)	Diameter of axial part (mm)	Diameter of nodular part (mm)
Tensile load test	6.8	25.7	1000	1500
Reciprocal load test	17.0	11.0	1000	1500

25.7m below ground level as tension test piles. For the reciprocal load test, piles were friction-cut down to 10.7m below ground level using the pipe-in-pipe method (i.e. double steel tube method). Figure 5 shows the relationship between the load and displacement at pile head in load test A. The maximum load for the tensile load test was 10,000kN, and the displacement at pile head under this condition was about 180mm. For the reciprocal load test, the maximum load was 16,000kN on the compressive side and 10,000kN on the tensile side; the displacement at pile head under such conditions was about 180mm on the compressive side and about 200mm on the tensile side.

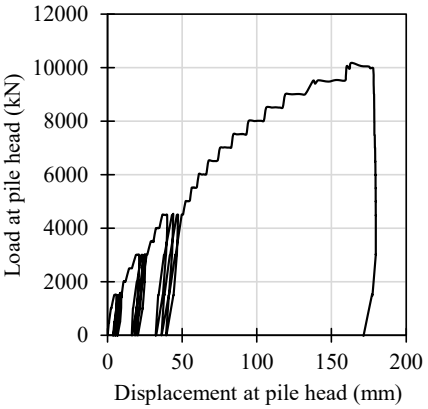

(a) Tensile load test

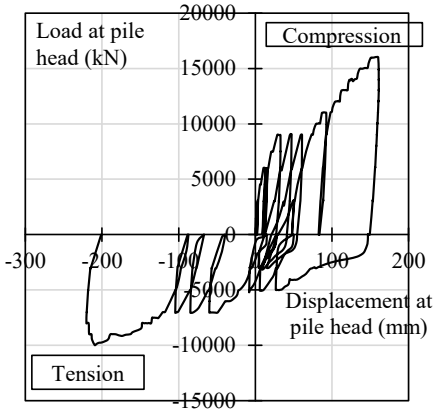

(b) Reciprocal load test

Figure 5 Load–displacement relationship at pile head (load test A)

Figure 6 shows the relationship between the bearing pressure and displacement at nodular part in load test A. The ultimate bearing pressure at nodular part in the tension test was about 7,000kN/m^2. The ultimate bearing pressure at nodular part in the reciprocal load test was about 2,000kN/m^2 for both the compressive and tensile sides. In all cases, the ultimate bearing pressure at nodular part was the value obtained for a displacement of about 10% of the diameter at nodular part (i.e., 150mm). It may be concluded that the failure of pile occurred at the nodular part in this load test.

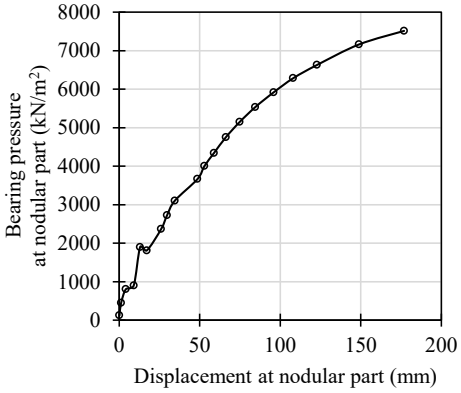

(a) Tensile load test

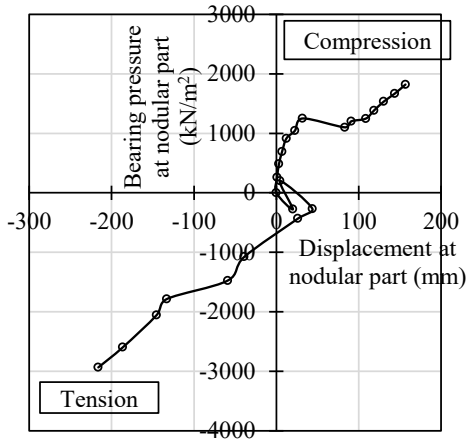

(b) Reciprocal load test

Figure 6 Bearing pressure–displacement relationship at nodular part (load test A)

3.3 Load Test B

Figure 7 and Table 2 outline load test B. A single test pile was used, and the noddular and end part of the pile were embedded in the diluvia sandy layer. A friction cut was performed down to about 6m below the ground surface using the pipe-in-pipe method (i.e. double steel tube method). The test consisted of a compressive load test and tensile load test that were performed on the same test pile. Figure 8 shows the relationship between the load and displacement at pile head in load test B. Although the compressive and tensile load tests were conducted separately in load test B, the relationships between the load and displacement at pile head are given in the same diagram.

The maximum compressive load was 28,000kN, and the displacement under this condition was about 180mm. The maximum tensile load was 6,000kN, and the displacement under this condition was about 270mm. Based on the residual displacement from compression, however, the displacement from tension was actually about 440mm. Figure 9 shows the relationship between the bearing pressure and displacement at nodular part in load test B. The ultimate bearing pressure at nodular part was about 6,500 and 700kN/m^2 for compressive and tensile load tests, respectively. In all cases, the ultimate bearing capacity was the value obtained for a displacement of about 10% of the diameter at nodular part (i.e., 150mm). It may be also concluded that the failure of pile occurred at the nodular part in this load test.

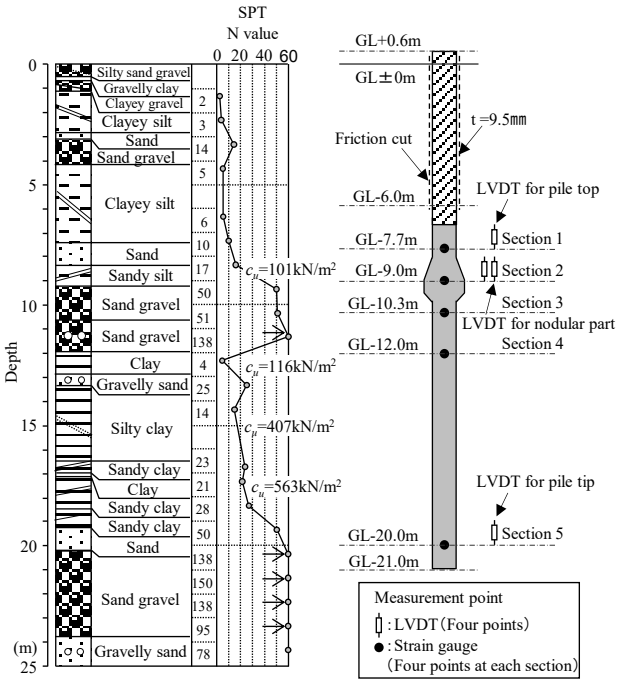

Figure 7 Summary of test piles and ground conditions (load test B)

Table 2 Specifications of test piles (load test B)

Load test	Pile length (m)	Depth of pile head (GL- m)	Diameter of axial part (mm)	Diameter of nodular part (mm)
Compressive load test Tensile load test	15.0	6.0	1000	1500

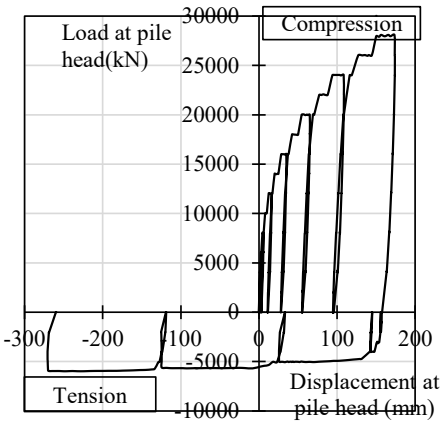

Figure 8 Load–displacement relationship at pile head (load test B)

4. RESULTS OF INVESTIGATION ON STANDARD BEARING CAPACITY

The standard bearing capacity was examined according to the concepts in the Railway Standards (Railway Technical Research Institute, 2012), where the maximum load was defined as the value when the displacement at the pile tip reached 10% of the pile diameter. Figure 10 shows the results of the investigation on the standard bearing capacity. The data were taken from two load tests

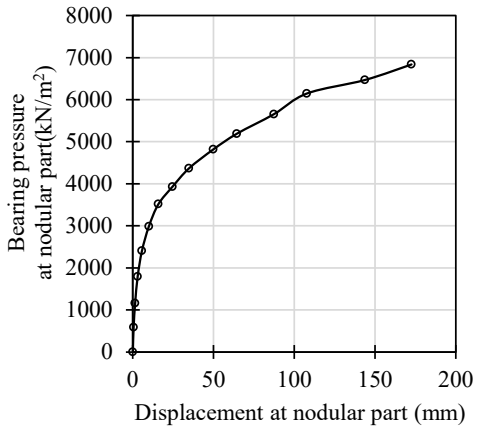

(a) Compressive load test

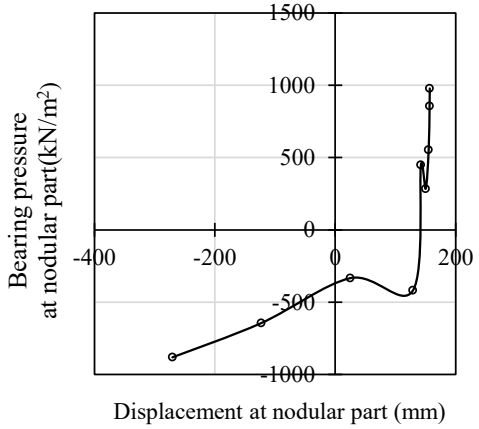

(b) Tensile load test

Figure 9 Bearing pressure–displacement relationship at nodular part (load test B)

in which piles were loaded with sufficient displacement (at least 10% of the pile diameter). The results of standard bearing capacity were categorized into the end bearing capacity, bearing pressure at nodular part, and shaft friction. The end bearing capacity was calculated by dividing the axial force reaching the pile tip by the pile tip area. The bearing pressure at the nodular part was calculated by dividing the difference in the axial forces above and below the nodular part by the horizontal projection area of the nodular part. Moreover, the shaft friction was calculated by dividing the difference in axial forces of each section by the peripheral area between the corresponding sections. Eqs. (1), (2-a) and (2-b) were used to estimate the standard bearing capacity of cast-in-place concrete piles according to the Railway Standards.

Standard end bearing capacity:

$$q_{tk} = 60\,N \text{ (kN/m}^2\text{)} \quad (1)$$

(Sandy soil: $q_{tk} \leq 3500$, gravel soil: $q_{tk} \leq 7500$)

Standard shaft friction (Sandy soil):

$$\gamma_{fk} = 3N\ (\leq 150) \text{ (kN/m}^2\text{)} \quad (2\text{-a})$$

Standard shaft friction (Clayey soil):

$$\gamma_{fk} = 6N\ (\leq 150) \text{ (kN/m}^2\text{)} \quad (2\text{-b})$$

where, N is the N value obtained from the standard penetration test.

Figure 10(a) shows the relationship between end bearing capacity, bearing pressure at nodular part and SPT N value. This figure also plots the standard end bearing capacity line for cast-in-place concrete piles as indicated by the Railway Standards. The end bearing capacity and bearing pressure at nodular part derived from the load tests of the nodular cast-in-place concrete piles form a relationship with values generally were the same or above the standard end bearing capacities provided by the Railway Standards. Figure 10(b) shows the relationship between the shaft friction and SPT N value. The standard shaft friction for cast-in-place concrete piles according to the Railway Standards is also plotted with the shaft friction. The calculated values from the equations provided by the Railway Standards were generally exceeded by the shaft friction obtained from the load tests of nodular cast-in-place concrete pile.

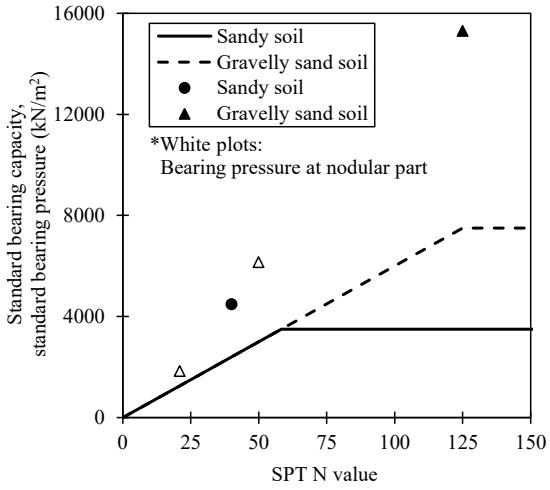

(a) Relationships between end bearing capacity, bearing pressure at nodular part and SPT N value

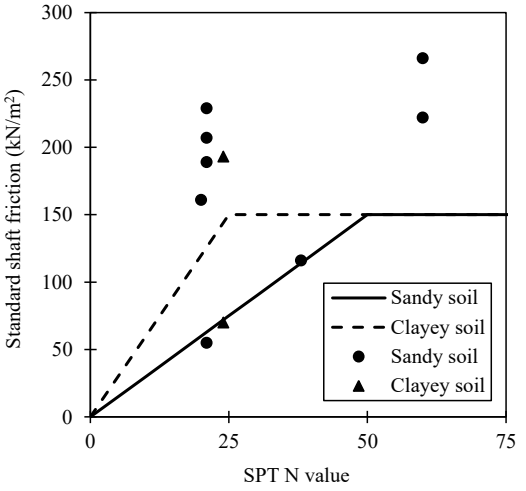

(b) Relationships between shaft friction and SPT N value

Figure 10 Design and tested bearing capacities

The shaft friction for cohesive soil was significantly lower than the standard shaft friction because the data were derived from the results of the tensile load test performed after the compression test and thus were subject to the effects of a significant deformation.

Figure 11 compares the calculated values for the standard bearing capacity using the bearing capacity formula as shown in Railway Standards and the observed values obtained from the load tests of nodular cast-in-place concrete pile. The observed values clearly exceeded the calculated values.

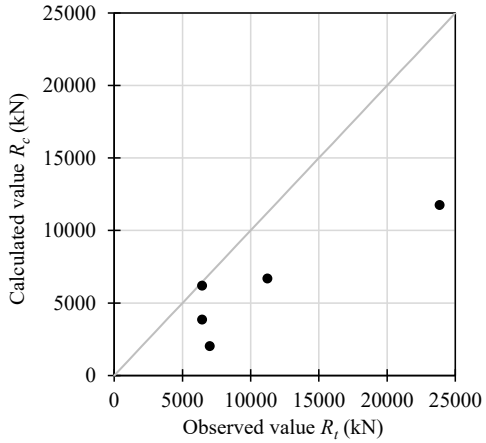

Figure 11 Relationship between calculated and observed values for design bearing capacity

5. CALCULATION OF GROUND RESISTANCE COEFFICIENT FOR NODULAR CAST-IN-PLACE CONCRETE PILE

5.1 Calculation method for ground resistance coefficient

The design vertical bearing capacity R_{vd} of a pile is calculated by using Eqs. (3) ~ (5) from the Railway Standards.

$$R_{vd} = f_r R_k = f_{rt} R_{tk} + f_{rf} R_{fk} \tag{3}$$

$$R_{tk} = q_{tk} A_t \tag{4}$$

$$R_{fk} = \gamma_{fk} U \Delta l \tag{5}$$

where, f_r: Ground resistance coefficient, R_k: Standard bearing capacity, f_{rt}: Ground resistance coefficient for pile end, R_{tk}: Standard end bearing capacity, f_{rf}: Ground resistance coefficient for pile shaft, R_{fk}: Standard shaft friction, q_{tk}: Standard end bearing capacity, A_t: Pile tip area, γ_{fk}: Standard shaft friction for different soil layers, U: Peripheral length of the pile, Δl: Length of different soil layers

Beside the standard bearing capacity, the ground resistance coefficient needs to be evaluated in order to calculate the design vertical bearing capacity with Eqs. (3) ~ (5). The ground resistance coefficients are stipulated to ensure that the prescribed reliability is secured for different required performance.

Let the actual measured values of the pile end resistance and shaft resistance when a certain limit state has been reached (i.e., the settlement has reached a certain standard displacement) in a vertical load test of a single pile be R_t^t and R_f^t, respectively. Then, the performance function Z for the action of the pile head load S can be expressed by Eq. (6) using R_t^t, R_f^t, and S as random variables. The subscript t indicates an actual measured value.

$$Z = R_t^t + R_f^t - S \tag{6}$$

The performance function Z generally becomes complex and it becomes difficult to easily derive the limit state exceedance probability. The first-order proximity reliability design method (i.e., first-order reliability method (FORM)) is used to approximate the probability variable with a normal distribution function, and a Taylor expansion is performed at the point where the performance function reaches zero (design point) to suspend the series with a first-order term. This allows linearization to be performed and the limit state exceedance probability to be calculated. If the performance function is expressed as a sum of the linearized normal distribution function when this method is used, then the limit state exceedance probability can be calculated without requiring convergence.

First, the probability variables R_t^t, R_f^t, and S are normalized using the characteristic values for the standard bearing capacities R_{tk} and R_{fk} and the characteristic value S_k of the load acting on the pile head. These are then assumed to be probability variables with mutually independent normal distributions. Then, the performance function Z given in Eq. (6) can be expressed as Eq. (7) by using the probability variables Y_t, Y_f, and Y_S. These have normal distributions for which the average value is 0 and stand-ard deviation is 1.

$$Z = R_{tk}\mu_t + R_{fk}\mu_f - S_k\mu_s + R_{tk}\sigma_t Y_t + R_{fk}\sigma_f Y_f - S_k\sigma_s Y_s \tag{7}$$

where, μ_t, μ_f, μ_s, σ_t, σ_f, σ_s: Average values and standard deviations of the probability variables

This transformation derives the point located at the shortest distance to the plane expressed by Eq. (7) from the origin located at (Y_t, Y_f, Y_s) as the design point. The safety index β can be derived with Eq. (8) and is defined as the shortest distance from the origin to the design point.

$$\beta = \frac{\mu_z}{\sigma_z} = \frac{R_{tk}\mu_t + R_{fk}\mu_f - S_k\mu_s}{\sqrt{(R_{tk}\sigma_t)^2 + (R_{fk}\sigma_f)^2 + (S_k\sigma_s)^2}} \tag{8}$$

If the standard probability variables are mutually independent according to the normal distribution function and if the performance function can be expressed as a linear function of the standard probability variables, then the safety index and limit state exceedance probability P_f ($Z \leq 0$) have the following relationship:

$$P_f = \Phi(-\beta) \tag{9}$$

where, Φ is a standard normal probability distribution function and expresses how far the average value, μ_z is located from the point at which the limit state is reached (Z=0) as a scale factor with respect to the standard deviation σ_z.

Table 3 lists the required performance and limit state necessary to calculate the ground resistance coefficient. Such values comply with the Railway Standards, and the five performance parameters were statistically analysed.

The ground resistance coefficient equivalent to the safety coefficient for the resisting side is derived by following the method described by Nishioka et al. (2008). The performance function in Eq. (6) can be expressed as Eq. (10) through a transformation that uses the ground resistance coefficients f_{rt} and f_{rf}, and activity coefficient γ_s

$$Z^d = f_{rt}R_{tk} + f_{rf}R_{fk} - \gamma_s S_k \tag{10}$$

Because Eq. (10) satisfies $Z^d = 0$ when the target safety index β_a is achieved, the ground resistance coefficient can be expressed by Eqs. (11-a) and (11-b).

$$f_{rt} = \mu_t - \beta_a \alpha_t \sigma_t \tag{11-a}$$

$$f_{rf} = \mu_f - \beta_a \alpha_f \sigma_f \tag{11-b}$$

where μ_t and μ_f: Average values of the probability variables, σ_t and σ_f: Standard deviations of the probability variables, β_a: Target safety index, α_t and α_f: Sensitivity coefficients

The target safety index β_a expresses the safety margin for respective limit states. Because the sensitivity coefficients α_t and α_f change in response to the change in the standard pile end bearing capacity ratio p_t, a ground resistance coefficient that reflects whether

Table 3 Required performance and limit state

(a) Excluding seismic motions

Required performance	Performance lists	Standard displacement (mm)	Target safety index β_a Exceedance probability of standard displacement P_f	Limit state
Usability	Long term bearing performance	20(13.3) ※1	β_a=1.6, P_f=5%	Crack by differential settlement
	Short term bearing performance	20	β_a=1.3, P_f=10%	
Safety	Stability	min(50 or 0.05D) ※2	β_a=1.0, P_f=16%	Noticeable displacement at railway

※1: The value in braket considering displacement increase of long term load test is used in statistical work. (Aoki et al., 1985)

※2: D means pile diameter.

(b) Seismic motions

Required performance	Performance lists	Standard displacement (mm)	Target safety index β_a Exceedance probability of standard displacement P_f	Limit state
Restorability and Performance level 1	Residual displacement	50 or 0.05D	β_a=0.85, P_f=20%	Maintenance and repair of railway
Restorability and performance level 2		0.1D	β_a=0.5, P_f=30%	Maintenance and repair of structure

the designed pile is a friction pile or bearing pile can be calculated. The sensitivity coefficients α_t and α_f and the standard pile end bearing capacity ratio p_t are given by Eqs. (12) ~ (14).

$$\alpha_t = p_t\sigma_t \Big/ \sqrt{p_t^2\sigma_t^2 + (1-p_t)^2\sigma_f^2} \tag{12}$$

$$\alpha_t = (1-p_t)\sigma_f \Big/ \sqrt{p_t^2\sigma_t^2 + (1-p_t)^2\sigma_f^2} \tag{13}$$

$$p_t = R_{tk} \big/ (R_{tk} + R_{fk}) \tag{14}$$

Because the average values μ_t, and μ_f are estimated from a small number of specimens, they are estimated from Eq. (15), which has a lower limit of 0.75 for the confidence level corresponding to the number of data points n.

$$\mu = \bar{\mu} - k_s\sigma \tag{15}$$

where, μ: Estimated average value, $\bar{\mu}$: Average value for the load test data, σ: Standard deviation of the load test data, k_s: Coefficient that corresponds to the number of data points n, as indicated in Figure 12.

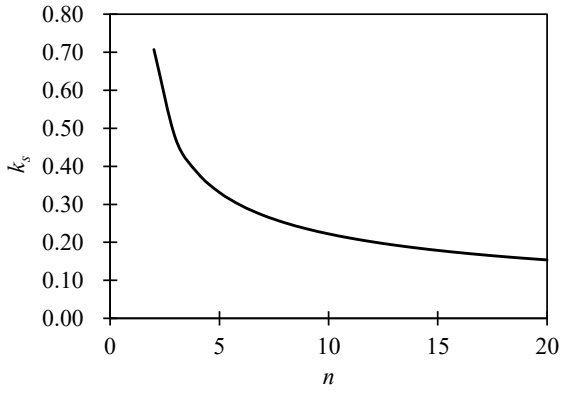

Figure 12 Coefficient k_s for data (confidence level: 0.75)

5.2 Calculation results for ground resistance coefficients for nodular cast-in-place concrete pile

Table 4 lists the average values and coefficients of variation of the statistical analysis. The table also presents the results of the statistical analysis for the cast-in-place concrete piles compared with the Railway Standards. The table inside the brackets next to the number of effective data points regarding the shaft friction is the total number of data points used for the investigation on the standard bearing capacity, as described in Section 4.1. The number of data points outside the brackets was adopted for the statistical analysis to eliminate data that contained significant effects from the loading history, such as the tensile load test implemented after the tension part of the alternating load test or the compression test that caused significant deformation.

Table 4 reveals that the cast-in-place concrete piles had a large coefficient of variation for the pile tip in the long term bearing performance with a small standard displacement. On the other hand, the nodular cast-in-place concrete piles tended to have smaller coefficients of variation at the pile tip and nodular part in the long term and short term bearing performance with a small standard displacement. This differed from the bearing capacity at the pile tip of the cast-in-place concrete piles, which are conventionally considered to have a large variance. This suggests that there is a small variance in the bearing capacity at the nodular part and pile tip sections of nodular cast-in-place concrete piles. The slime treatment using a slime cleaner specially made for the nodular part and the replacement of the slurry with a better liquid after the slime treatment may be reasons for this tendency. The pile shaft can be conservatively evaluated by applying the same evaluation as that for the cast-in-place concrete piles because the coefficients of variation related to the pile shaft were also smaller than those of the cast-in-place concrete piles.

The target safety index in Table 1 and the statistical values and standard pile end bearing capacity ratios in Table 2 were then used to calculate the ground resistance coefficient using the method described in Section 4.2. It is necessary to consider the uncertainties of the ground survey in actual designs, even for the statistical values with smaller coefficients of variation (less than 30%) in Table 2. For the purpose of comparison, the procedures in the Railway Standards were followed. Thus, even when the coefficients of variation were under 30%, they were still considered to be 30% for the purpose of this report.

Figure 13 shows the relationship between the ground resistance coefficient and standard pile end bearing capacity ratio. The ground resistance coefficient f_r is used to calculate the design bearing capacity as shown in Eq. (3). From the bottom to the top, each line represents the ground resistance coefficients for different required performance: the usability and long term bearing performance, usability and short term bearing performance, safety and non-seismic motions, restorability and performance level 1, and restorability and performance level 2.

Figure 13 also shows the ground resistance coefficients for cast-in-place concrete piles as described by the Railway Standards with dotted lines for the purpose of comparison. For the required performance, the ground resistance coefficient tended to be small when the standard pile end bearing capacity ratio was large. The ground resistance coefficients were generally larger than those of the cast-in-place concrete piles because the average values were

Table 4 Resistance factors for nodular cast-in-place concrete pile

		Pile shaft				Pile tip or Pile tip + nodular part（Nodular cast-in-place concrete pile）			
	Required performance	Usability	Usability	Safety / Restorability and performance level 1	Restorability and performance level 2	Usability	Usability	Safety / Restorability and performance level 1	Restorability and performance level 2
	Performance lists	Long term bearing performance	Short term bearing performance	Stability Residual displacement	Residual displacement	Long term bearing performance	Short term bearing performance	Stability Residual displacement	Residual displacement
	Standard displacement	Long term20mm	20mm	min (50mm, 5%D)	10%D	Long term20mm	20mm	min (50mm, 5%D)	10%D
Cast-in-place concrete pile	Effective data number n	7	6	6	6	9	8	8	8
	Average value μ	1.16	1.16	1.31	1.37	0.5	0.56	0.85	1.39
	Variation coefficient V	38%	38%	40%	33%	60%	46%	44%	49%
Nodular cast-in-plsce concrete pile	Effective data number n	3 (5)	3 (5)	3 (5)	3 (5)	2	2	2	2
	Average value μ	1.06	1.22	1.62	1.74	0.63	0.73	1.06	1.35
	Variation coefficient V	21%	16%	25%	65%	22%	27%	41%	65%

greater and the standard deviations were smaller. For the restorability and performance level 2, the average value of the pile shaft was sufficiently larger than those of the cast-in-place concrete piles. However, because the coefficients of variation were large, the ground resistance coefficients were about the same in regions where the standard pile end bearing capacity ratio was small. The values were lower than those of the cast-in-place concrete piles in the region where the standard pile end bearing capacity ratios were large because the coefficients of variation were large. This is despite the fact that the average values for the pile end and nodular part were about the same as those of the cast-in-place concrete piles.

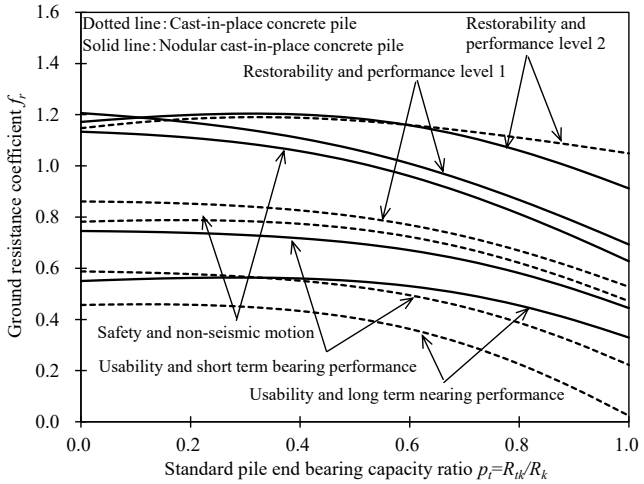

Figure 13 Ground resistance coefficient for nodular cast-in-place concrete pile

The ground resistance coefficients of the nodular cast-in-place concrete piles were inferred to be about the same as those of the cast-in-place concrete piles when the slime treatment using a slime cleaner specially made for the nodular part was not performed or when the slurry was not replaced with better liquid after the slime treatment. The ground resistance coefficients were believed to increase with the bearing resistance in the nodular part when the above construction process was performed.

6. CONCLUSIONS

This paper presents the results of standard bearing capacity and the evaluation of the bearing capacity for nodular cast-in-place concrete piles. The results are summarized as follows.

1) The calculation formula for the standard bearing capacity of cast-in-place concrete piles described in the Railway Standards was compared with the data from load tests on nodular cast-in-place concrete piles. The bearing capacity of the nodular cast-in-place concrete piles was found to be comparable to the values from the standard bearing capacity calculation formula for cast-in-place concrete piles de-scribed by the Railway Standards.
2) The ground resistance coefficients for nodular cast-in-place concrete piles were calculated in compliance with the Railway Standards. The results showed that they generally exceeded the ground resistance coefficients of the cast-in-place concrete piles.
3) The ground resistance coefficients were believed to increase with the bearing capacity in the nodular cast-in-place concrete pile. This suggests that the slime treatment using a slime cleaner specially made for the nodular part and the replacement of the slurry with a better liquid after the slime treatment may be reasons for this tendency.

7. REFERENCES

Watanabe, K. 2008. Static axial reciprocal and tensile load tests of single cast-in-place concrete nodular piles (Part 1 to 4). Proceedings of Annual National Conference of Architectural Institute of Japan:567-576. (in Japanese).

Watanabe, K. et al. 2009. Static axial tensile and compressive load tests of nodular diaphragm wall supporting high-rise tower (Part 1 to 5). Proceedings of Annual National Conference of Architectural Institute of Japan: 439-450. (in Japanese).

Watanabe, K. et al. 2010. Static Axial Compressive and Tensile Load Test of Single Cast-in-place Nodular Concrete Pile (Part 1 to 4). Proceedings of Annual National Conference of Architectural Institute of Japan: 613-620. (in Japanese).

Watanabe, K. et al. 2012. Static load tests of nodular cast-in-place concrete pile and estimation on resistance of nodular part. Proceedings of IS-Kanazawa: 749-756.

The Japanese Geotechnical Society. 2002. JGS standard, Method for Axial Load Test of Single Piles. (in Japanese).

Railway Technical Research Institute. 2012. Design Standards for Railway Structures and Commentary. (in Japanese).

Nishioka, H. et al. 2008. Calculation of bearing capacity by pile construction methods using statistical analysis of load test data. Railway Technical Research Institute Report: Vol. 22, No. 10, 41-46. (in Japanese).

Aoki, K. et al. 1985. Coefficient of subgrade reaction used in design of piles. Structural Design Documents: No. 83, 20-25. (in Japanese).